

Microwave synthesis and characterization of organophilic clay/polyacrylic-g-polycarbonate nanocomposites

S. Pandey¹, S. Mahtab¹, S. K. Gururani², M. G. H. Zaidi^{1*}

¹ Department of Chemistry, G. B. Pant University of Agriculture & Technology, Pantnagar-Utraakhanda-263 145, India

² Department of Chemistry, M.B. Post Graduate College, Kumaun University, Nainital-263 631, India

Received: April 10, 2023; Revised: August 10, 2023

Polymer nanocomposites (PNCs) were synthesized through graft copolymerization of polyacrylic acid onto polycarbonate followed by solution intercalation of organophilic montmorillonite (OMMT) into graft copolymer under microwave irradiation. PNCs were characterized through diverse spectral, thermal methods and scanning electron microscopy (SEM). Formation of PNCs was ascertained through UV-visible, FTIR spectra, X-ray diffraction and scanning electron microscopy. The matrix of the graft copolymer has been found to contain microparticulate distributions of OMMT, leading to the formation of PNCs. Simultaneous thermogravimetric-differential thermal analysis-differential thermogravimetry reveals moderate thermal stability of PNCs.

Keywords: Polymer nanocomposites, Graft copolymerization, Montmorillonite, Characterization.

INTRODUCTION

Recently, there has been an increased interest in development of polymer nanocomposites (PNCs), involving phyllosilicates for their potential applications in environmental cleanup [1], packaging, aerospace, and automotive industries [2-4]. Montmorillonite (MMT) belongs to the family of smectite clay holding 2:1 phyllosilicates arrangement comprising two tetrahedral sheets along with one octahedral sheet of aluminosilicates. MMT has received enormous attention over decades as the inexpensive phyllosilicates as filler for development of PNCs [5-6]. The high abundance, and rich intercalation chemistry allows MMT to serve as preferred choice for designing of two-dimensional PNCs [7]. Majority of thermoplastic and thermosetting polymers are hydrophobic and are not compatible with MMT. In order to afford the enhanced binding with polymers matrix, treatment of clays with surfactants offers a viable method to achieve their enhanced reinforcement into polymer matrix to develop the PNCs with improved barrier properties, structural rigidity, heat resistance, flame retardancy, superhydrophobicity, promising mechanical, dynamic mechanical behavior and antimicrobial activities [8].

Chemical pretreatment of clays is well established methods to develop the organophilic clays as fillers for development of PNCs [5-7]. The

viable pretreatment leads in presence of amino acids, organic quaternary ammonium salts, tetra organic phosphonium halides as modifiers for clay materials [5]. Functional amphiphilic graft polymers has been considered as compatibilizers to achieve the PNCs with key examples of polyethylene-graft-polymethacrylic acid [8], polystyrene (PS)-graft-cellulose [9], PS-graft-cellulose acetate [10], syndiotactic PS-g-polymethyl methacrylate [11], starch-g-PS [12].

Over the years, MW irradiation-based polymer manufacturing has gained popularity as a quick, efficient, and environmentally benign method of producing polymer products. Microwave treatment offers the dielectric way of heating where molecules bearing permanent dipole moment align to the applied electromagnetic field, resulting in rotation, friction, and collision of molecules that facilitates polymerization reactions [13, 14]. The present investigation deals with MW-assisted synthesis of (PAA)-g-polycarbonate (PC) and its solution intercalation with organophilic montmorillonite (OMMT) to afford the PNCs. In this process, OMMT was synthesized through cation exchange of commercially available MMT (K10) with cetyl pyridinium bromide (CPBr) in [14]. Synthesized PAA-g-PC and respective PNCs were characterized through diverse spectral, thermal methods and scanning electron microscopy [15-17].

* To whom all correspondence should be sent:
E-mail: smiitr@gmail.com, mgh_zaidi@yahoo.com

EXPERIMENTAL

Starting materials

Acrylic acid and PC (Tg. 150-160°C, density 1.2 g/cc at 25 °C) were procured from Sigma Aldrich Chemicals. Azobisisobutyronitrile (AIBN), Na-MMT (K-10) and cetyl pyridinium bromide (CPBr) were procured from Himedia, India. AIBN was re-crystallized from methanol and dried under reduced pressure at room temperature (mp 102-104°C). Other chemicals and solvent (purity > 99%) were locally arranged and used without further purification. OMMT was prepared through dispersing Na-MMT (2.0 g) in de-ionized water (800 ml) followed by sonication over 1h. A solution of CPBr (20 mL, 0.36 M) in water was slowly added into the suspension of MMT under sonication (500 W) over 1 hr. OMMT was then isolated through filtration from the suspension and washed several times with distilled water until the testing of the mother liquor with AgNO₃ (0.1 M) showed negative test for silver bromide. OMMT was dried overnight at 110°C and ground to pass a 400-mesh sieve. The % yield and % G 47.50 and 18.50 of PAA-g-PC was deduced according to the reported procedure and was found as 47.50 and 18.50, respectively [7].

MW-assisted synthesis of PNCs

AA (2.90×10^{-2} mole/dl), PC (1.0 g) and AIBN (1.21×10^{-3} mol/dl) were dissolved in dichloromethane (5 ml) in a 100 mL-borosilicate glass vial and irradiated under MW at 100W over 5 min. The PC-g-PAA was isolated through successive washing of the crude product several times with methanol followed by filtration till achieving the uniform weight of the solid residue. The isolated PC-g-PAA (1.0 g) was subsequently subjected to solution intercalation in presence of OMMT (5 phr) in dichloromethane (25 ml) under MW irradiation at 100W over 5 min. The PNCs were isolated in 98 % yield through removal of dichloromethane followed by drying at 50 °C/ 400 mmHg over 3 h. PAA was also synthesized under similar reactions conditions and used as reference for comparing the results.

Characterization

Uv-visible spectra were recorded in methanol on a Genesis 10 Thermospectronic spectrophotometer in tetrahydrofuran. FTIR spectra were recorded on Galaxy 300 Mattson FT-IR infrared spectrometer in KBr disks. XRD spectra were recorded at 25°C on a Rigaku-Geiger flex diffractometer using Cu-K α radiation ($\lambda = 0.154056$). The crystallite size of OMMT and gallery spacing of OMMT was deduced through Debye Scherer method [16]. Thermograms were recorded on Perkin Elmer Pyris Diamond

thermal analyzer at sample size ranging in N₂@ 10 °C/min with reference to alumina. SEM were recorded on JEOL-JSM-6610LV. TEM was recorded on JEOL 1011 (Tokyo, Japan) instrument with a primary beam voltage of 80 kV.

RESULTS AND DISCUSSION

Spectra

UV spectra reveal characteristic absorption maxima (nm) for PC (a), PC-g-PAA (b) and PNCs (c) at 266, 269 and 264 respectively (Fig. 1). The carboxylate functionalities extended by acrylic acid contribute red shift to the absorption of PC in the respective PC-g-PAA, whereas PNCs have shown a blue shift over graft copolymers due to binding of the OMMT with functionalities of the graft-copolymers [17].

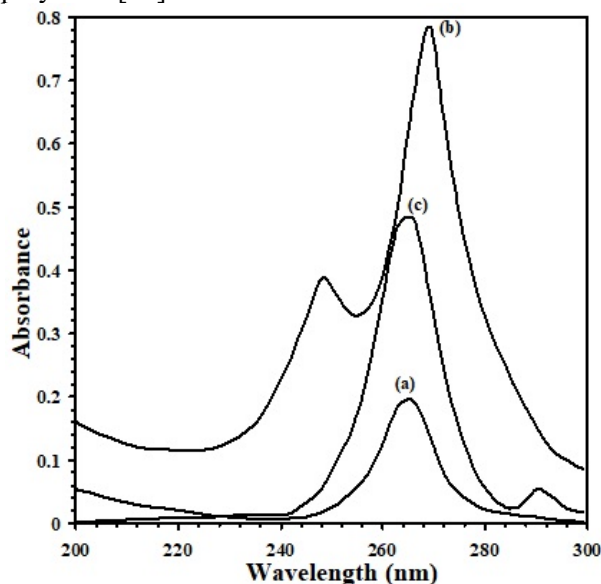


Fig. 1. UV spectra of PC (a), PC-g-PAA (b) and PNCs

Fig.2 demonstrates the FTIR spectra of OMMT (a), PC (b), PAA-g-PC (c) and PNCs (d).

FTIR spectrum of OMMT reveals the characteristic wave numbers (cm⁻¹) corresponding to 3396.93 (ν OH), 3004.35 (ν Ar. C-H), 2918.61 (ν CH₂, as.), 2852.09 (ν CH₂, sy.), 1630.43 (δ OH), 1481.72 (δ CH₂, scissoring), 1373.91 (δ CH₃, as.), 1317.39 (δ CH₃, sy.), 1169.57-1040.07 (ν Si-O), 782.61-717.39 (ρ CH₂), 673.91 (δ Si-O), 523.50 (ν Si-O/Si-O-Al), 465.31 (ν Si-O/Si-O-Fe) (Fig. 2a) [14]. PC shows wave numbers at 3784(ν COOH), 3439.7(ν O-H), 2360(ν C-H, as.CH₂), 1632.9 (δ , H₂O), 771.1(ρ C-H) (Fig. 2b) [17]. PAA-g-PC shows wave numbers at 3895.3 (ν C=O), 3022.3-2926.3(ν =C-H, CH₂), 2360.9(ν (C-H, as, CH₂), 1654.6(δ , H₂O), 1216.9 (ν C-O-C, as), 1027.6 (ν C-O), 929.2 (ν C...O), 764 (ρ C-H) (Fig. 2c). PNCs shows wave numbers at 3747.4-3600.5 (ν

C=O), 3021.7(ν =C-H, CH₂), 2925.4 (ν CH₃ as), 2854.2 (ν CH₂ sy), 1652.5(δ H₂O), 1216.4(ν C-O-C, as), 1017.4(ν C-O), 928.8(ν C...O) and 762.6(ρ C-H). This was associated with additional functionalities corresponding to 520.50 (ν Si-O/Si-O-Al), 450.31 (ν Si-O/Si-O-Fe), which reveals the formation of PNCs[14].

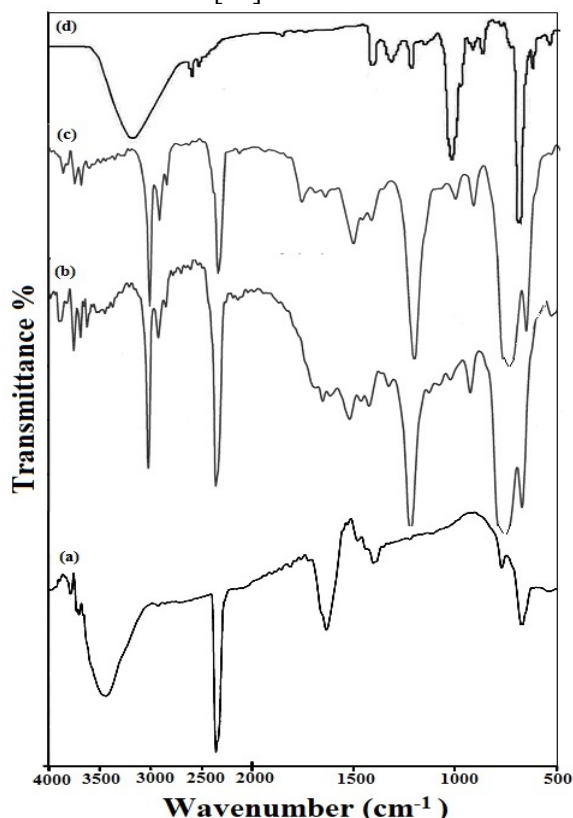


Fig. 2. FTIR spectra of OMMT (a), PC(b), PAA-g-PC (c) and PNCs (d)

Microstructure

XRD spectrum of OMMT reveals its amorphous characteristics with appearance of characteristic

indexing of 2θ at 24.01° (001), 22.76° (005), 19.57° (02; 11), 27.47° (007) (Fig. 3a) [14,18]. XRD spectrum of PC demonstrates the characteristic crystalline zone at 2θ (d) corresponding to 14.54 (6.07). The indexing appeared at 3.46 (25.69) and 2.03 (31.44) attributes to semi-crystalline zones of PC (Fig. 3b). PC, PC-g-PAA (Fig. 3c) and PNCs (Fig. 3d) reveals common peaks ranging $2\theta=21$ to 24° corresponding to the van der Waals distance of neighboring polymer chains segments [20]. The indexing at 14.54 (6.07) and 15.15 (5.82) attributes to reduction in gallery spacing of PC due to graft copolymerization. The appearance of (001) indexing in the range of $2\theta=21$ to 28 attributes to binding of OMMT with PAA-g-PC.

TEM images reveal the formation of spherical micro particles of OMMT with particle size ranging 10 to 55 nm (Fig. 4a). The crystallite size of OMMT deduced from Debye Scherer methods (48 nm) is in closed agreement to particle size deduced from TEM (Fig. 4a). The samples for SEM imaging were made through cast of their films in dichloromethane. In order to have the comparable results, all the SEM images were recorded at 1000X, 10 μ m. The cast films of PC reveal occasional appearance of air pockets due to evaporation of dichloromethane during their formation (Fig. 4b). PC-g-PAA reveals characteristic phase separation due to immiscibility of PAA into PC phase (Fig. 4c) [19]. PNCs has shown random distribution of assemblies of OMMT agglomerates into PC matrix (Fig. 4d).

Thermal stability

Fig. 5 demonstrates the simultaneous TG-DTA-DTG curves for PC (a), PAA (b), PAA-g-PC (c) and PNCs (d). The color codes for TG, DTA and DTG curves are black, green and violet. The pertinent thermal data are summarized in Table 1.

Table 1. Thermal data deduced PC, PAA, PAA-g-PC and respective PNCs from thermograms

| Sample | M ^A | TG | | DTG | | | DTA |
|----------|----------------|-------------|------------|-----------------------------|-----------------------------|-----------------|-------------------------------|
| | | Onset | Endset | R ₁ ^b | R ₂ ^c | PT ^d | $-\Delta H$ (SV) ^e |
| PC | 0.29 | 94.64 (431) | 0.26 (600) | 1.22 (448) | 1.51 (479) | 586 | 3168 (54.0) |
| PAA | 2.20 | 89.50 (199) | 0.10 (536) | 0.63 (244) | 0.59 (587) | 499 | 2140 (63.6) |
| PC-g-PAA | 1.50 | 90.90 (200) | 0.00 (552) | 0.55 (235) | 0.21 (523) | 511 | 1820 (40.4) |
| PNCs | 4.5 | 86.87 (200) | 9.61 (500) | 0.62 (240) | 0.82 (400) | 407 | 4400 (35.2) |

A: Moisture content (wt%); B : Rate of thermal decomposition at first step; C; Rate of thermal decomposition at second step; D: DTA peak temperature (°C); E: $-\Delta H$ (SV)^e =Enthalpy of thermal decomposition in mJ/mg (DTA signal voltage in μ V)

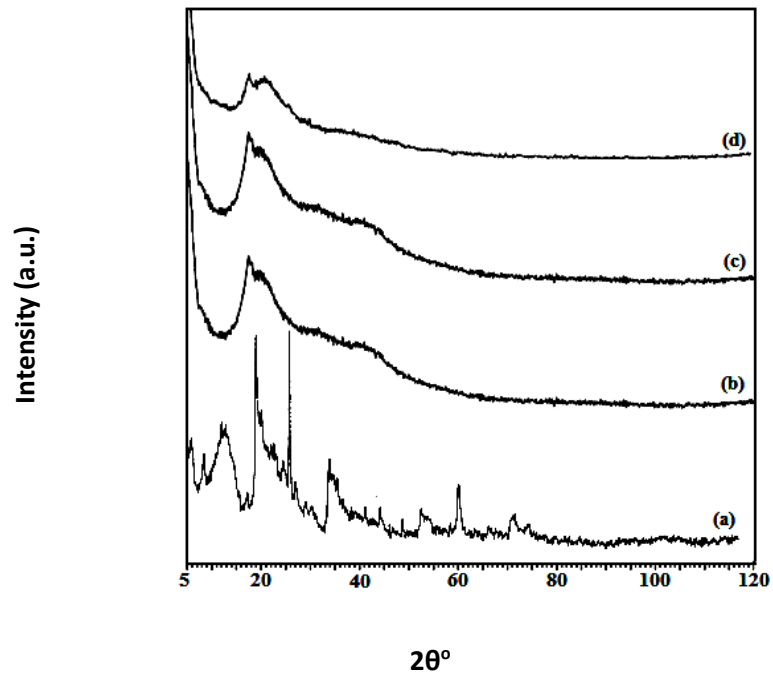


Fig. 3. XRD spectra of OMMT (a), PC (b), PAA-g-PC(c) and PNCs (d)

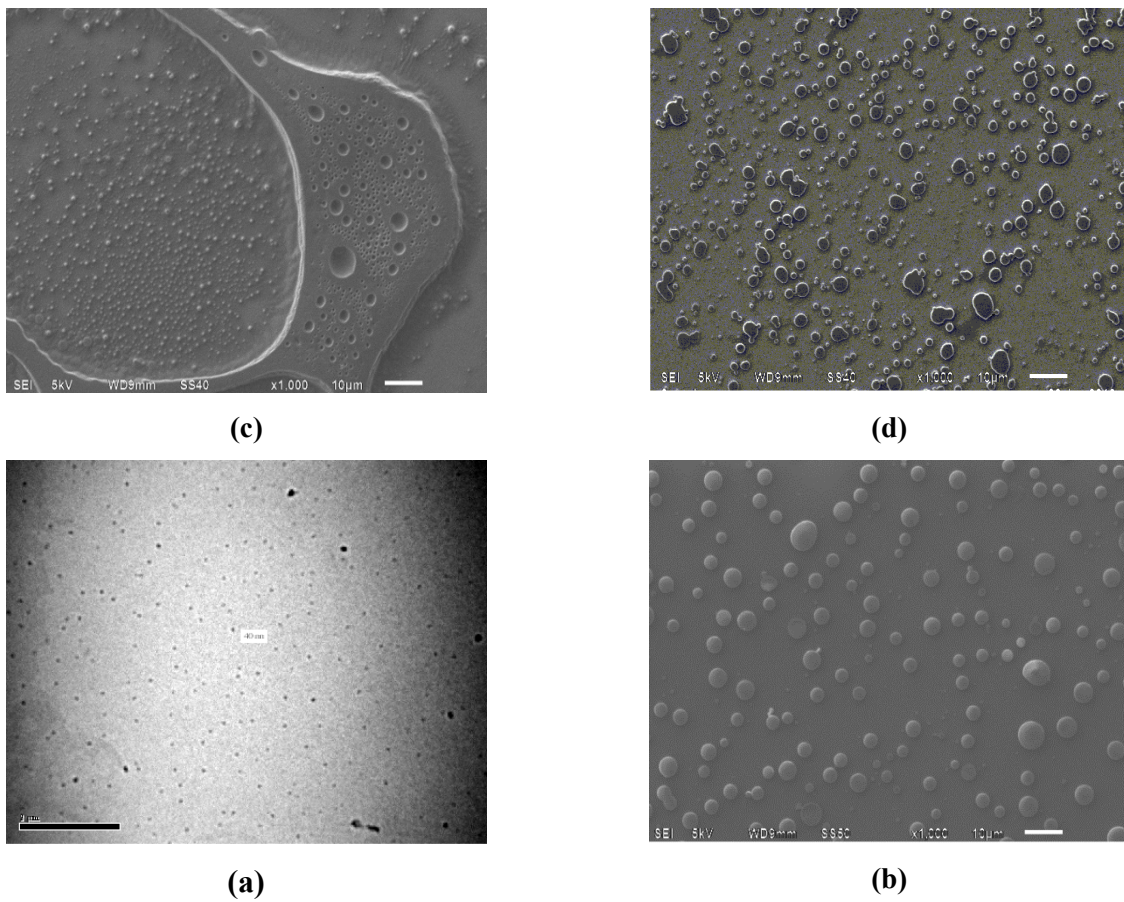


Fig. 4. TEM of OMMT (a).SEM of PC (b), PAA-g-PC (c) and PNCs (d)

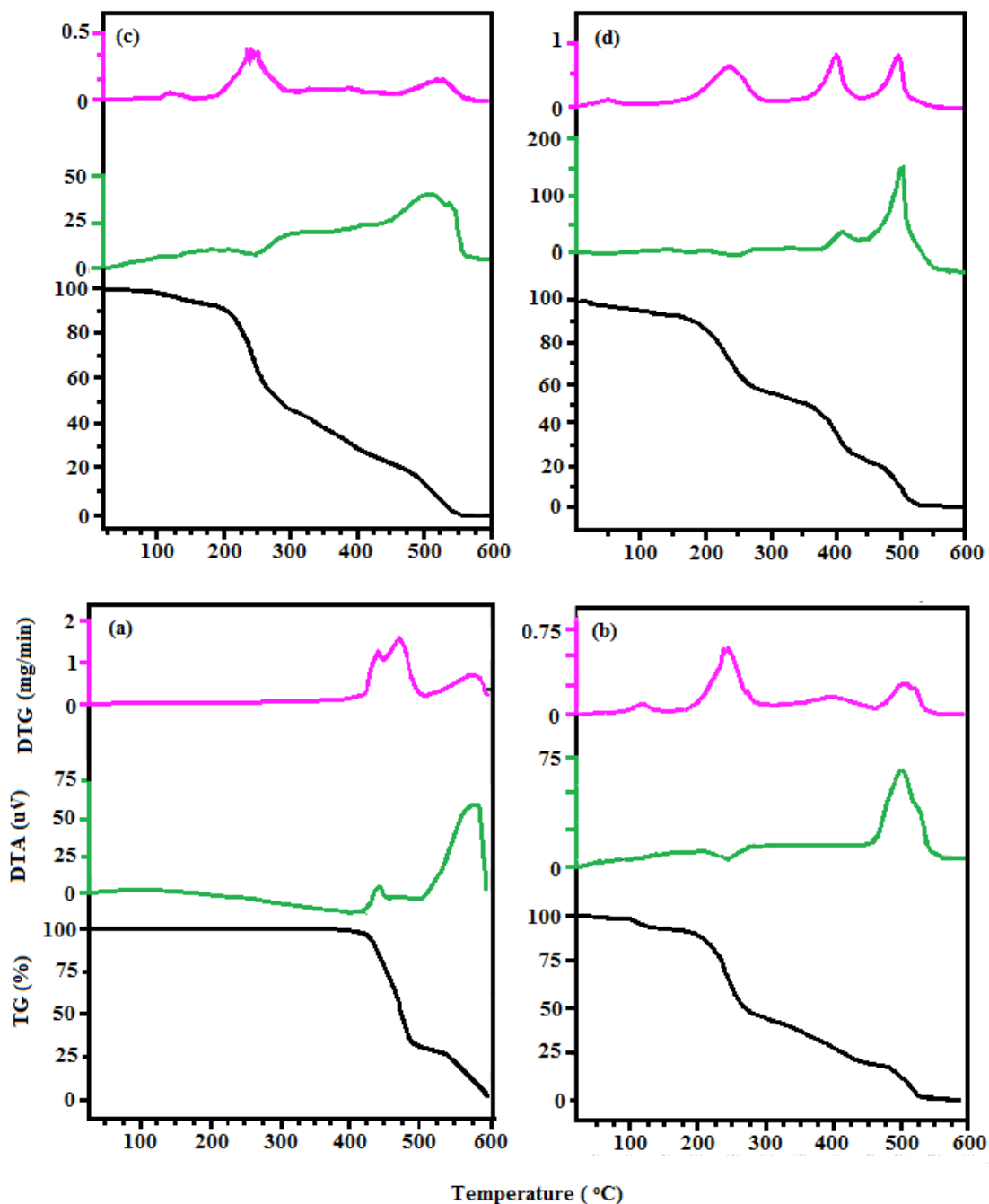


Fig. 5. Simultaneous TG-DTA-DTG of PC (a), PAA (b), PAA-g-PC (c) and PNCs (d). The color codes for TG, DTA and DTG are black, green and violet.

TG reveals two step decompositions by all the samples. Graft copolymerization of PAA onto PC and onward modification of PAA-g-PC with OMMT has liberated the PNCs with moderately improved thermal stability. PC shows TG onset at 431 °C leaving 94.64% Wr (weight residue). Prior TG onset, the 0.29 wt% loss at 100°C attributes to the moisture content associated with PC. DTG reveals two stage decomposition of PC at 448 °C and 479 °C with respective degradations (mg/min) @ 1.22 and 1.51. Thermal decomposition of PC has rendered the

exothermic DTA at 54 μ V with evolution of -3168 mJ/mg of heat at 586 °C.

PAA was decomposed with TG onset at 199 °C leaving 89.50% Wr. Due to the inherent hygroscopic nature of PAA, has rendered enhanced moisture content (2.20 wt%). Decomposition of PAA was concluded at TG endset of 536 °C, leaving 0.10% Wr. DTG reveals the major decomposition of PAA at 244 °C and 587 °C @ (mg/min) 0.63 and 0.59, respectively.

Thermal decomposition of PAA has rendered the exothermic DTA at 63.6 μ V with evolution of -2140 mJ/mg of heat at 499 °C. The high moisture content of PAA-g-PC (1.50 wt %) over PC (0.29 wt%) is due to the grafting of the hygroscopic macromolecular signets over PC. No significant change in TG onset and corresponding W_r % of PAA-g-PC and respective PNCs was observed over PAA. However, PAA-g-PC was completely volatilized at 552 °C due to inferior thermal stability [21]. DTG reveals usual two step decomposition of PAA which were initiated at 235 °C and 553 °C @ (mJ/mg) 0.55 and 0.21 respectively. PAA-g-PC (500 °C) has rendered a substantial reduction in TG onset over PC (600 °C). However, the controlled rate of degradation of PAA-g-PC revealed through DTA indicates their enhanced thermal stability of PC [17]. Thermal decomposition of PAA-g-PC has rendered the exothermic DTA at 40.41 μ V with evolution of -1820 mJ/mg of heat at 523 °C.

The contribution of OMMT as a thermal stabilizer for PAA-g-PC was revealed at TG endset appeared at 500 °C leaving 9.61% W_r by PNCs. The high moisture content of PNCs (4.5 wt%) probably attributes to the insignificant loading of OMMT. However, high % W_r (9.61) at TG endset (500 °C) attributes to moderate thermal stability of PNCs over PAA-g-PC, PAA and PC respectively. However, the second step decomposition appeared of PNCs was progressed @0.82 mg/min, that was relatively higher over PC and PAA-g-PC. PNCs was exothermically decomposed with DTA at 35.20 μ V leaving 4400mJ/mg of heat at 407 °C. Thermograms reveals that grafting of PAA onto PC and their onward modification with OMMT has rendered PNCs with enhanced moisture uptake (4.5 wt%) without any improving in TG onset temperatures over PAA. Thermal stability of PNCs was moderately compromised at TG endset. However, the highest liberation of heat (4400 mJ/mg) reveals the thermal stability of PNCs prior to their TG endset.

CONCLUSION

The present investigation demonstrates a clean, rapid and viable process of synthesis of polymer nanocomposites under microwave irradiation at 100W. The process involves microwave assisted synthesis of polyacrylic acrylic-graft-polybisphenol A-carbonate (PAA-g-PC) with graft yield and efficiency of 47.50% and 18.50, followed by their solution intercalation with organophilic montmorillonite (OMMT). For this purpose, OMMT was synthesized through cationic exchange of cetyl

pyridinium bromide with montmorillonite (K 10). The crystallite size of OMMT deduced from XRD (48 nm) was in closed agreement with transmission electron microscopy data (~55 nm). Diverse spectral and thermal methods revealed the formation of OMMT, PAA-g-PC and respective PNCs. Scanning electron microscopy revealed the random distribution of the microparticles of OMMT into the matrix of PAA-g-PC. PNC has shown moderate thermal stability over PC and respective PAA-g-PC.

REFERENCES

1. M. Hanmate, A. K. Pulikkal, *Chemosphere*, **307** (2), 135869 (2022).
2. M. Okamoto, *Poly. Nanocompos. Eng.*, **4** (1), 457 (2023).
3. S. Gul, A. Kausar, B. Muhammad, S. Jabeen, *Polym. Plast. Technol. Eng.*, **55** (3), 684–703 (2016).
4. F. Guo, S. Aryna, Y. Han, Y. Jiao, *Appl. Sci.*, **8** (9), 1696 (2018).
5. S. L. Bee, M. A. A. Abdullah, S. T. Bee, L. T. Sin, A. R. Rahmat, *Prog. Polym. Sci.* **85** (5), 57 (2018).
6. S. Pandey, M.G.H. Zaidi. S. K. Gururani, *Sci. J. Rev.*, **2** (11), 296 (2013).
7. R. Wang, H. Li, G. Ge, N. Dai, J. Rao, H. Ran, Y. Zhang, *Mol.*, **26** (9), 2521 (2021).
8. N. Sibold, C. Dufour, F. Gourbilleau, M. N. Metzner., C. Lagreve, L. L. Pluart, P. J. Madec, T. N. Pham, *Appl. Clay Sci.*, **38** (1-2), 130 (2007).
9. S. Murugesan, T. Scheibel, *Adv. Funct. Mater.*, **30** (17), 190801 (2020).
10. M. Abbasian, M. Bakshi, M. Jaymand, S. G. Karaj-Abad, *J. Elast. Plast.*, **51** (5), 473 (2019).
11. G. Moreira, E. Fedeli, F. Ziarelli, D. Capitani, L. Mannia, L. Charles, S. Viel, D. Gignes, C. Lefy, *Polym. Chem.*, **6** (3), 5244 (2015).
12. M. Jaymand, *Polym. J.*, **43** (2), 901 (2011).
13. H. Namazi, A. Dadkhah, M. Mosadegh, *J. Polym. Environ.*, **20** (3), 794 (2012).
14. R. Hoogenboom, U. S. Schubert, *Macromol. Rapid Commun.*, **28** (6), 368 (2007).
15. H. Negi, T. Agarwal, M. G. H. Zaidi, A. Kapri, R. Goel, *Biotech. J.*, **6** (1):107 (2010).
16. T. Agarwal, K. A. Gupta, M. G. H. Zaidi, *J.Chem. Chem. Eng.*, **55** (3):62 (2012).
17. S. Mehtab, M. G. H. Zaidi, P. Joshi, D. Bawari, *IOP Sci. Notes*, **1**, 034201(2020).
18. S. K. Joshi, J. C. Kapil, A. K. Rai, M. G. H. Zaidi, *Physica Status Solidi*, **199** (2): 321 (2003)
19. A. S. Pakdaman, J. Morshedian, Y. Jahani, *J. Appl. Polym. Sci.*, **127** (2), 1211 (2013).
20. M. Spirkova, J. Pavlicevic, A. Strachota, R. Poreba, O. Bera, L. Kapralkova, J. Idrian, M. Slouf, M. Ladic, J. Budinski, *Eur. Polym. J.*, **47** (3), 235 (2011).
21. D. Debier, A. M. Jonas, R. Legras, *J. Polym. Sci. B*, **36** (5), 2197 (1987).
22. V. Agarwal, M. G. H. Zaidi, S. Alam, A. K. Rai *Int. J. Polym. Anal. Charact.*, **14** (1), 52 (2009).